

# Search for $2\beta$ decay of $^{106}\text{Cd}$ with enriched $^{106}\text{CdWO}_4$ crystal scintillator in coincidence with four HPGe detectors

P. Belli<sup>a</sup>, R. Bernabei<sup>a,b,1</sup>, V.B. Brudanin<sup>c</sup>, F. Cappella<sup>d</sup>, V. Caracciolo<sup>d</sup>,  
 R. Cerulli<sup>d</sup>, D.M. Chernyak<sup>e</sup>, F.A. Danevich<sup>e</sup>, S. d'Angelo<sup>a,b,2</sup>, A. Di Marco<sup>a,b</sup>,  
 A. Incicchitti<sup>f,g</sup>, M. Laubenstein<sup>d</sup>, V.M. Mokina<sup>e</sup>, D.V. Poda<sup>e,h</sup>, O.G. Polischuk<sup>e,f</sup>,  
 V.I. Tretyak<sup>e,f</sup>, I.A. Tupitsyna<sup>i</sup>

<sup>a</sup>*INFN, sezione di Roma "Tor Vergata", I-00133 Rome, Italy*

<sup>b</sup>*Dipartimento di Fisica, Università di Roma "Tor Vergata", I-00133 Rome, Italy*

<sup>c</sup>*Joint Institute for Nuclear Research, 141980 Dubna, Russia*

<sup>d</sup>*INFN, Laboratori Nazionali del Gran Sasso, I-67100 Assergi (AQ), Italy*

<sup>e</sup>*Institute for Nuclear Research, MSP 03680 Kyiv, Ukraine*

<sup>f</sup>*INFN, sezione di Roma, I-00185 Rome, Italy*

<sup>g</sup>*Dipartimento di Fisica, Università di Roma "La Sapienza", I-00185 Rome, Italy*

<sup>h</sup>*Centre de Sciences Nucléaires et de Sciences de la Matière, 91405 Orsay, France*

<sup>i</sup>*Institute of Scintillation Materials, 61001 Kharkiv, Ukraine*

## Abstract

A radiopure cadmium tungstate crystal scintillator, enriched in  $^{106}\text{Cd}$  to 66%, with mass of 216 g ( $^{106}\text{CdWO}_4$ ), was used to search for double beta decay processes in  $^{106}\text{Cd}$  in coincidence with four ultra-low background high purity germanium detectors in a single cryostat. New improved limits on the double beta processes in  $^{106}\text{Cd}$  have been set on the level of  $10^{20} - 10^{21}$  yr after 13085 h of data taking. In particular, the half-life limit on the two neutrino electron capture with positron emission,  $T_{1/2}^{2\nu\varepsilon\beta^+} \geq 1.1 \times 10^{21}$  yr, has reached the region of theoretical predictions. With this half-life limit the effective nuclear matrix element for the  $2\nu\varepsilon\beta^+$  decay is bounded as  $M_{eff}^{2\nu\varepsilon\beta^+} \leq 1.1$ . The resonant neutrinoless double electron captures to the 2718 keV, 2741 keV and 2748 keV excited states of  $^{106}\text{Pd}$  are restricted at the level of  $T_{1/2} \geq (8.5 \times 10^{20} - 1.4 \times 10^{21})$  yr.

PACS number(s): 29.40.Mc, 23.40.-s

*Keywords:* Double beta decay,  $^{106}\text{Cd}$ , Low counting experiment, Scintillation detector, HPGe detector

---

<sup>1</sup>Corresponding author. *E-mail address:* rita.bernabei@roma2.infn.it.

<sup>2</sup>Deceased

# 1 INTRODUCTION

Experiments to search for neutrinoless double beta ( $0\nu 2\beta$ ) decay are considered as a promising way to study properties of neutrino and weak interactions, test the lepton number conservation [1, 2, 3]. In addition, the process can be mediated by right-handed currents in weak interaction, existence of massless (or very light) Nambu-Goldstone bosons (majorons), and many other effects beyond the Standard Model [1, 3, 4, 5].

Experimental efforts are concentrated mainly on the double beta decay with emission of two electrons (see reviews [6, 7, 8, 9, 10, 11, 12, 13]). The results of the experiments to search for double beta processes with decrease of nuclear charge: the capture of two electrons from atomic shells ( $2\varepsilon$ ), electron capture with positron emission ( $\varepsilon\beta^+$ ), and emission of two positrons ( $2\beta^+$ ) are substantially more modest (we refer reader to the reviews [6, 7, 14] and references 11–27 in [15]). Even the allowed two neutrino mode of the double beta plus processes is not yet detected unambiguously: there are only indications on two neutrino double electron capture in  $^{130}\text{Ba}$  [16, 17] and  $^{78}\text{Kr}$  [18] with the half-lives on the order  $10^{20} - 10^{21}$  yr. At the same time a strong motivation to search for neutrinoless  $\varepsilon\beta^+$  decay is related with the possibility to refine the mechanism of the  $0\nu 2\beta^-$  decay when observed: whether it appears due to the Majorana mass of neutrino or due to the contribution of the right-handed admixtures in the weak interaction [19]. In addition, experimental data on the two neutrino decay could be useful to improve theoretical calculations of the decay probability.

The isotope  $^{106}\text{Cd}$  (energy of decay  $Q_{2\beta} = 2775.39(10)$  keV [20], natural isotopic abundance  $\delta = 1.25(6)\%$  [21]) is one of the most suitable nuclei to search for the double beta plus processes. In addition the isotope  $^{106}\text{Cd}$  is favored to search for resonant  $0\nu 2\varepsilon$  transitions to excited levels of  $^{106}\text{Pd}$  when there is a coincidence between the released energy and the energy of an excited state [15, 22]. The decay scheme of  $^{106}\text{Cd}$  is presented in Fig. 1.

The nuclide  $^{106}\text{Cd}$  is one of the most studied (see a detailed review of the previous investigations in [15]). At present there are three experiments in progress aiming at search for double beta decay of  $^{106}\text{Cd}$ . The TGV-2 experiment in the Modane underground laboratory in France utilizes 32 planar HPGe detectors with 16 thin foils of enriched  $^{106}\text{Cd}$  ( $\delta = 75\%$ ) installed between the detectors. Recently new enriched foils with a higher isotopic concentration of  $^{106}\text{Cd}$   $\delta = 99.6\%$  were installed. The sensitivity of the experiment is at the level of  $\lim T_{1/2} \sim 10^{20}$  yr [24, 25, 26]. The main advantage of the TGV-2 experiment is a high sensitivity to the  $2\nu 2K$  decay of  $^{106}\text{Cd}$  with the theoretically shortest half-life of the three allowed channels.

The COBRA experiment uses an array of CdZnTe room temperature semiconductors  $\approx 1$  cm<sup>3</sup> each at the Gran Sasso underground laboratory in Italy. The sensitivity of the experiment to the double beta processes in  $^{106}\text{Cd}$  is at the level of  $\lim T_{1/2} \sim 10^{18}$  yr [27].

The third experiment, also carried out at the Gran Sasso laboratory, utilizes a radiopure cadmium tungstate crystal scintillator with mass 216 g produced from cadmium enriched in  $^{106}\text{Cd}$  to 66% ( $^{106}\text{CdWO}_4$ ) [28]. At the first stage of the experiment the sensitivity at the level of  $\lim T_{1/2} \sim 10^{20} - 10^{21}$  yr was reached for different channels of double beta decay of  $^{106}\text{Cd}$  [15]. To increase the experimental sensitivity to the  $2\beta$  processes with emission of  $\gamma$  quanta, the  $^{106}\text{CdWO}_4$  scintillator was placed inside a low background HPGe detector with four Ge crystals. Here we report the final results of the experiment with the  $^{106}\text{CdWO}_4$  scintillation detector operated in coincidence (anticoincidence) with the four crystals HPGe  $\gamma$  detector. Preliminary results of the experiment were presented in conference proceedings [29, 30, 31, 32].

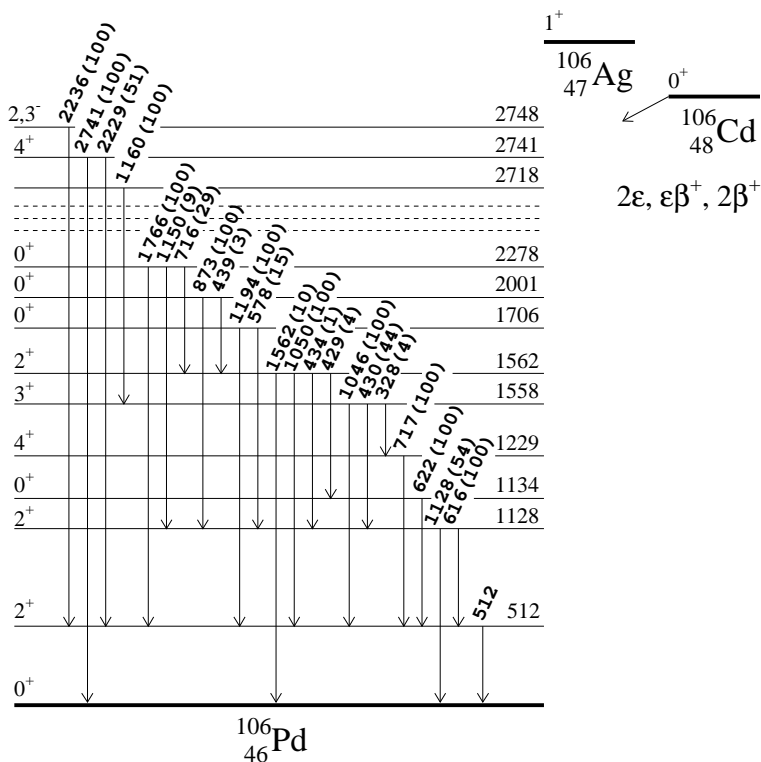


Figure 1: Simplified decay scheme of  $^{106}\text{Cd}$  [23] (levels at 2283–2714 keV are omitted). Energies of the excited levels and of the emitted  $\gamma$  quanta are in keV. Relative intensities of  $\gamma$  quanta are given in parentheses.

## 2 THE EXPERIMENT

The  $^{106}\text{CdWO}_4$  crystal scintillator was viewed through a lead tungstate ( $\text{PbWO}_4$ ) crystal light-guide ( $\varnothing 40 \times 83$  mm) by 3 inches low radioactive photomultiplier tube (PMT) Hamamatsu R6233MOD (see Fig. 2). The  $\text{PbWO}_4$  crystal was developed from deeply purified [33] archaeological lead [34]. The detector was installed in an ultra-low background GeMulti HPGe spectrometer of the STELLA (SubTERRanean Low Level Assay) facility [35] at the Gran Sasso underground laboratory of the INFN (Italy) at the depth of 3600 m of water equivalent. Four HPGe detectors of the GeMulti set-up are mounted in one cryostat with a well in the centre. The volumes of the HPGe detectors are approximately 225 cm<sup>3</sup> each.

An event-by-event data acquisition system is based on two four-channel digital spectrometers (DGF Pixie-4, XIA, LLC). One device (marked (1) in Fig. 2) is used to provide spectrometric data for the HPGe detectors, while the second Pixie-4 (2) acts as a 14-bit waveform digitizer to acquire signals from the  $^{106}\text{CdWO}_4$  detector at the rate of 18.8 MSPS over a time window 54.8  $\mu\text{s}$ . The second Pixie-4 unit records also trigger signals from the home made unit SST-09, which provides the triggers only if the signal amplitude in the  $^{106}\text{CdWO}_4$  detector exceeds  $\sim 0.6$  MeV to avoid acquisition of a large amount of data caused by the decays of  $^{113}\text{Cd}^m$  ( $Q_\beta = 586$  keV) present in the  $^{106}\text{CdWO}_4$  crystal [15, 36]. The signals from the timing outputs of the HPGe detectors after summing are fed to the third input of the second Pixie-4 digitizer to select coincidence between the  $^{106}\text{CdWO}_4$  and HPGe detectors off-line.

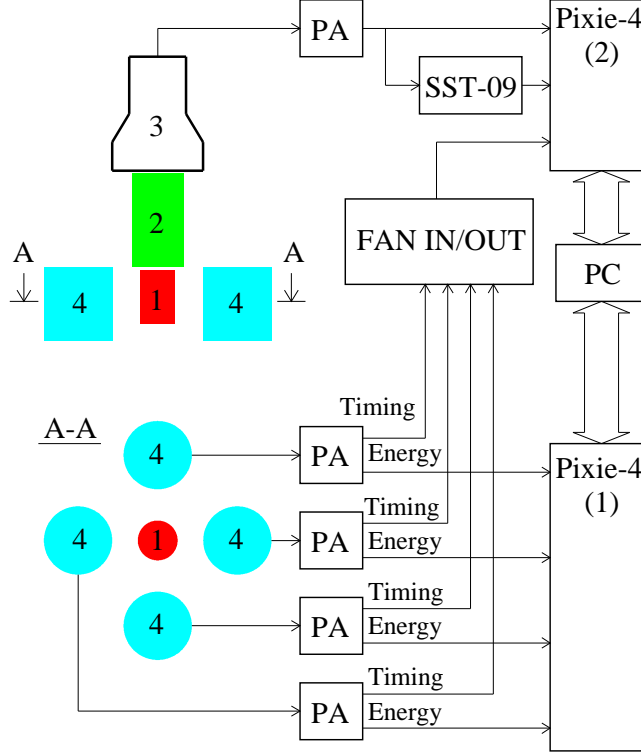


Figure 2: (Color online) Low background  $^{106}\text{CdWO}_4$  crystal scintillator (1) viewed through  $\text{PbWO}_4$  light-guide (2) by PMT (3). The scintillator is installed between HPGe detectors (4). Scheme of the electronic chain: (PA) preamplifiers; (FAN IN/OUT) linear FAN-IN/FAN-OUT; (SST-09) home-made electronic unit to provide triggers for cadmium tungstate scintillation signals; (Pixie-4) four-channel all digital spectrometers; (PC) personal computer.

The  $^{106}\text{CdWO}_4$  and HPGe detectors were calibrated with  $^{22}\text{Na}$ ,  $^{60}\text{Co}$ ,  $^{137}\text{Cs}$  and  $^{228}\text{Th}$   $\gamma$  sources. The energy resolution of the  $^{106}\text{CdWO}_4$  detector can be described by the function:  $\text{FWHM} = (21.7 \times E_\gamma)^{1/2}$ , where FWHM and  $E_\gamma$  are given in keV. The energy resolution of the HPGe detectors during the experiment was  $\text{FWHM} \approx 2 - 3$  keV for the 1332 keV  $\gamma$  quanta of  $^{60}\text{Co}$ .

Energy spectrum and distribution of the start positions of the  $^{106}\text{CdWO}_4$  detector pulses relatively to the HPGe signals accumulated with the  $^{22}\text{Na}$   $\gamma$  source (see upper panel in Fig. 3) demonstrate presence of coincidences between the  $^{106}\text{CdWO}_4$  and HPGe detectors under the condition that the energy of events in the HPGe detectors is equal to 511 keV (energy of annihilation  $\gamma$  quanta), while practically there is no coincidence in the data accumulated with  $^{137}\text{Cs}$ . As one can see in Fig. 3, the distributions simulated by the EGS4 code [37] are in agreement with the experimental data obtained with  $^{22}\text{Na}$ ,  $^{137}\text{Cs}$  and  $^{228}\text{Th}$  gamma sources. It should be stressed that the energy threshold of the  $^{106}\text{CdWO}_4$  detector in the coincidence mode ( $\approx 50$  keV) is much lower than that in the anticoincidence mode since the data acquisition in the coincidence mode is triggered by the signals in the HPGe detectors.

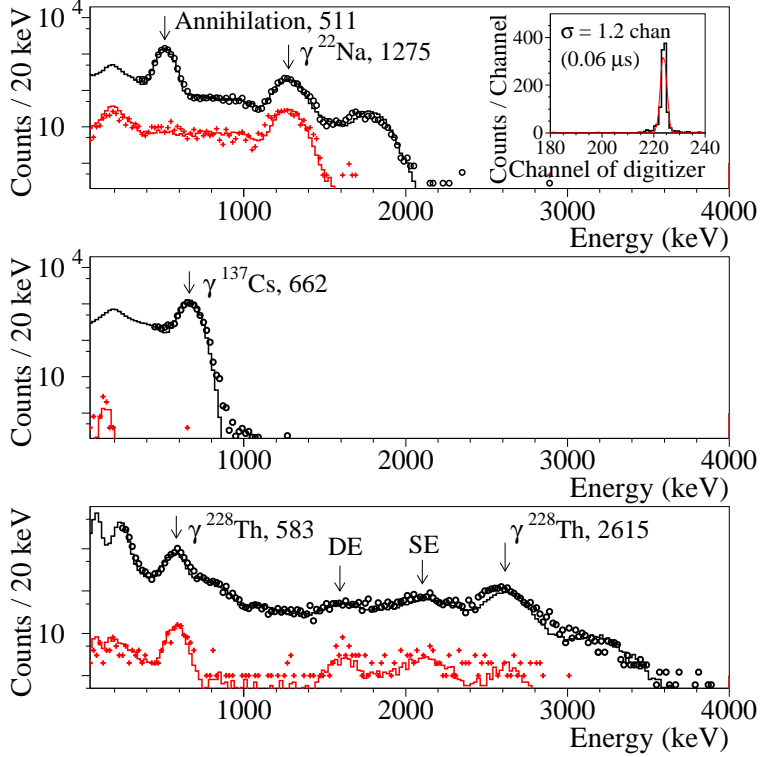


Figure 3: (Color online) Energy spectra of  $^{22}\text{Na}$  (upper figure),  $^{137}\text{Cs}$  (middle figure) and  $^{228}\text{Th}$  (lower figure)  $\gamma$  sources accumulated by the  $^{106}\text{CdWO}_4$  detector: with no coincidence (black circles), and in coincidence with energy 511 keV in the HPGe detector (red crosses). The data simulated by using the EGS4 Monte Carlo code are drawn by solid lines. (Inset) Distribution of the  $^{106}\text{CdWO}_4$  detector pulses start positions relatively to the HPGe signals with the energy 511 keV accumulated with  $^{22}\text{Na}$  source (the time shift of the  $^{106}\text{CdWO}_4$  signals by  $\simeq 220$  channels is due to the tuning of the digitizer to provide baseline data).

## 3 RESULTS AND DISCUSSION

### 3.1 Data analysis

The mean-time pulse-shape discrimination method (see, e.g., [38]) was used to discriminate  $\gamma(\beta)$  events from  $\alpha$  events caused by internal contamination of the crystal by uranium and thorium. The scatter plot of the mean time versus energy of the background events accumulated over 571 h by the  $^{106}\text{CdWO}_4$  detector is depicted in Fig. 4. The efficiency of the pulse-shape discrimination is worse than that in the previous experiment [15] due to the lower light collection efficiency with the  $\text{PbWO}_4$  light-guide. Nevertheless, the distribution of the mean time for the events with energies in the range 0.9 – 1.1 MeV (see Inset in Fig. 4) justifies pulse-shape discrimination between  $\alpha$  particles and  $\gamma$  quanta ( $\beta$  particles). The mean time for  $\gamma$  quanta was measured with the  $^{228}\text{Th}$   $\gamma$  source in the energy range 0.5 – 2.6 MeV as  $\tau_\gamma = 9843$ . The energy dependence of the mean time distribution sigma ( $\sigma_\gamma^\tau$ ) was determined as  $\sigma_\gamma^\tau = 3376/\sqrt{0.1 \times E_\gamma}$ , where  $E_\gamma$  is energy of gamma quanta in keV. The pulse-shape discrimination was also used to reject overlapped pulses (mainly caused by pileups of the  $^{113}\text{Cd}^m$   $\beta$  decay events) and pileups

of the  $\text{PbWO}_4$  scintillation signals (characterized by rather short decay time at the level of  $\approx 0.3 \mu\text{s}$  [38]) with the  $^{106}\text{CdWO}_4$  signals (effective average decay time  $\approx 13 \mu\text{s}$  [39]).

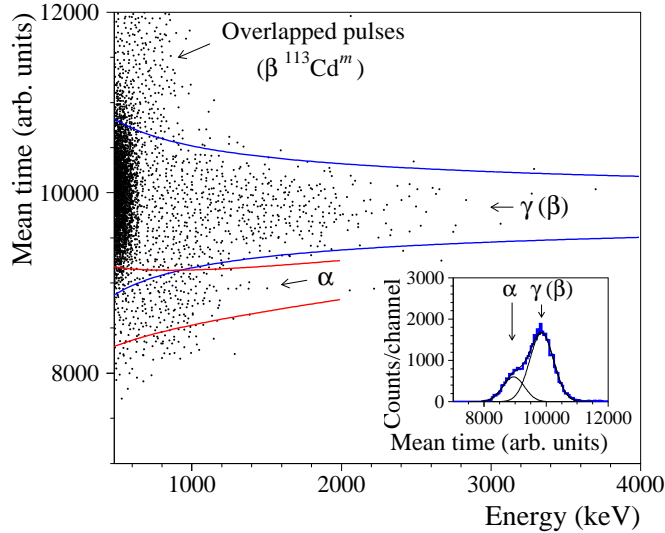


Figure 4: (Color online) Mean time (see text) versus the energy accumulated over 571 h with the  $^{106}\text{CdWO}_4$  crystal scintillator in the low-background set-up. The plus-minus two sigma interval for mean time values corresponding to gamma quanta (beta particles) and one sigma interval for alpha particles are depicted. Events with the mean time values greater than  $\approx 1.1 \times 10^4$  can be explained by the overlap of events (mainly of beta decays of  $^{113}\text{Cd}^m$  in the crystal). Inset: Distribution of the mean times in the energy interval 0.9 – 1.1 MeV demonstrates the ability of pulse-shape discrimination between  $\gamma(\beta)$  and  $\alpha$  events.

The energy spectra accumulated over 13085 h by the  $^{106}\text{CdWO}_4$  detector in anticoincidence with the HPGGe detectors, in coincidence with event(s) in at least one of the HPGGe detectors with energy  $E > 200$  keV,  $E = 511$  keV and  $E = 1160$  keV are presented in Fig. 5. The events in the anticoincidence spectrum were selected by using the following cuts: 1) there is no signal(s) in the HPGGe detectors, 2) the mean time ( $\tau$ ) value of a scintillation pulse is within the plus-minus two sigma interval around the central value:  $\tau_\gamma - 2\sigma_\tau < \tau < \tau_\gamma + 2\sigma_\tau$  (the interval is shown in Fig. 4). The pulse-shape discrimination cut selects 95.5% of  $\gamma(\beta)$  events. The spectrum of the  $^{106}\text{CdWO}_4$  detector in coincidence with the energy release in at least one of the HPGGe detectors of more than 200 keV was built with the help of the same pulse-shape discrimination cut. The energy spectra of the  $^{106}\text{CdWO}_4$  detector in coincidence with the signal(s) in the HPGGe detectors with energy 511 keV (1160 keV) were built by using the following cuts: 1) there is event(s) in at least one of the HPGGe detectors with energy  $E = 511 \pm 3\sigma_{511}$  keV ( $E = 1160 \pm 2.3\sigma_{1160}$  keV) where  $\sigma_{511}$  and  $\sigma_{1160}$  are the energy resolutions of the HPGGe detectors for the annihilation peak and for gamma quanta with energy 1160 keV, respectively; 2) the signals in the  $^{106}\text{CdWO}_4$  and HPGGe detectors coincide within the plus-minus three sigma time interval (see Inset of Fig. 3, the time cut selects 99.7% of the coinciding events); 3) the mean time value of a  $^{106}\text{CdWO}_4$  scintillation pulse is within the  $\pm 3\sigma_\tau$  interval. The pulse-shape discrimination cut selects 99.7% of the  $\gamma(\beta)$  events.

The data accumulated by the  $^{106}\text{CdWO}_4$  detector in anticoincidence with the HPGGe detectors confirmed the assumption about surface contamination of the  $^{106}\text{CdWO}_4$  crystal by  $^{207}\text{Bi}$

[15]. The  $\gamma$  peaks of  $^{207}\text{Bi}$  observed in [15] disappeared after the cleaning of the scintillator by potassium free detergent and ultra-pure nitric acid.

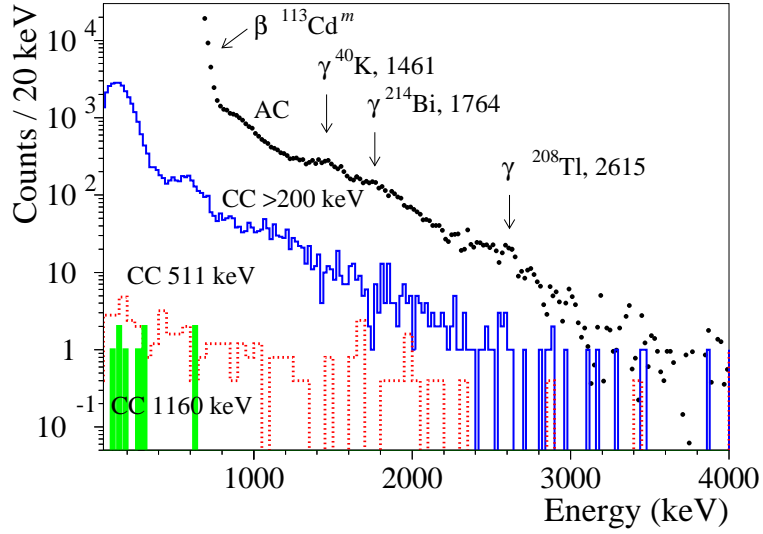


Figure 5: (Color online) Energy spectra of  $\gamma$  and  $\beta$  events accumulated over 13085 h by the  $^{106}\text{CdWO}_4$  detector in anticoincidence with the HPGe detectors (“AC”), in coincidence with event(s) in at least one of the HPGe detectors with the energy  $E > 200$  keV (“CC  $>200$  keV”),  $E = 511 \pm 3\sigma_{511}$  keV (“CC 511 keV”), and  $E = 1160 \pm 2.3\sigma_{1160}$  keV (“CC 1160 keV”).

The anticoincidence spectrum was fitted in the energy interval 940 – 3980 keV ( $\chi^2/\text{n.d.f.} = 157/118 = 1.33$ , where n.d.f. is the number of degrees of freedom) by the model built from the energy distributions simulated by EGS4 code [37]. The model includes radioactive contamination of the  $^{106}\text{CdWO}_4$  crystal scintillator [15, 36], external gamma quanta from the materials of the set-up ( $^{40}\text{K}$ ,  $^{232}\text{Th}$ ,  $^{238}\text{U}$  in the cryostat of the HPGe detector, PMT,  $\text{PbWO}_4$  light-guide,  $^{26}\text{Al}$  in the aluminium well of the cryostat), distribution of alpha particles (which passed the pulse-shape discrimination cut to select beta and gamma events), cosmogenic  $^{110}\text{Ag}^m$  in the  $^{106}\text{CdWO}_4$  scintillator and two neutrino  $2\beta^-$  decay of  $^{116}\text{Cd}$  with the half-life  $T_{1/2} = 2.62 \times 10^{19}$  yr [40] present in the  $^{106}\text{CdWO}_4$  crystal with the isotopic abundance  $\delta = 1.5\%$  [28]. The result of the fit and the main components of the background are shown in Fig. 6.

The energy spectrum accumulated by the HPGe detector is presented in Fig. 7 together with the background data taken over 4102 h. The counting rate of the HPGe detector with the  $^{106}\text{CdWO}_4$  detector inside exceeds slightly the background counting rate. Some excess (at the level of 30% – 170% depending on the energy of  $\gamma$  quanta) is observed in the peaks of  $^{214}\text{Bi}$  and  $^{214}\text{Pb}$  (daughters of  $^{226}\text{Ra}$  from the  $^{238}\text{U}$  family). We assume that the excess is due to the radioactive contamination of the  $^{106}\text{CdWO}_4$  detector and due to the HPGe detector passive shield modification (some part of the passive shield was removed to install the  $^{106}\text{CdWO}_4$  detector). We have also observed gamma quanta with energy 1809 keV, which we ascribe to cosmogenic  $^{26}\text{Al}$  in the aluminium well of the cryostat. Besides, there is a clear peak at the energy 262.5(5) keV with the counting rate 0.381(4) counts/hour (the peak is shown in the middle part of Fig. 7). We ascribe the peak to gamma quanta of the isomeric transition of  $^{113}\text{Cd}^m$  with energy 263.7(3) keV [41].

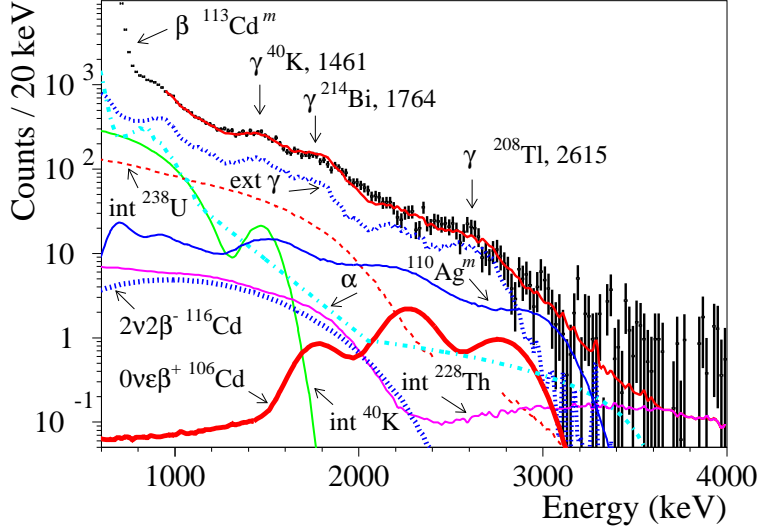


Figure 6: (Color online) The energy spectrum of the  $\gamma$  and  $\beta$  events accumulated over 13085 h in the low background set-up with the  $^{106}\text{CdWO}_4$  crystal scintillator (points) together with the background model (red continuous superimposed line). The main components of the background are shown: the distributions of internal and external ("ext  $\gamma$ ")  $^{40}\text{K}$ ,  $^{232}\text{Th}$  and  $^{238}\text{U}$ , distribution of residual alpha particles ( $\alpha$ ), cosmogenic  $^{110}\text{Ag}^m$  in the  $^{106}\text{CdWO}_4$  scintillator (with activity 0.3 mBq/kg) and  $2\nu 2\beta^-$  decay of  $^{116}\text{Cd}$ . The excluded distribution of the  $0\nu\varepsilon\beta^+$  decay of  $^{106}\text{Cd}$  to the ground state of  $^{106}\text{Pd}$  with the half-life  $T_{1/2} = 1.5 \times 10^{21}$  yr is shown too.

### 3.2 Limits on $2\beta$ processes in $^{106}\text{Cd}$

The response functions of the  $^{106}\text{CdWO}_4$  and HPGe detectors to the  $2\beta$  processes in  $^{106}\text{Cd}$  were simulated with the help of the EGS4 code. The simulated energy distributions in the  $^{106}\text{CdWO}_4$  detector without coincidence and in coincidence with 511 keV  $\gamma$  quanta (in coincidence with 622 keV gamma quanta for the  $2\nu 2\varepsilon$  and  $2\nu\varepsilon\beta^+$  decays to the 1134 keV excited level of  $^{106}\text{Pd}$ ) in the HPGe detector are presented in Fig. 8.

There are no peculiarities in the data accumulated with the  $^{106}\text{CdWO}_4$  and HPGe detectors that could be ascribed to the  $2\beta$  processes in  $^{106}\text{Cd}$ . Therefore only lower half-life limits can be set by using the formula:

$$\lim T_{1/2} = \ln 2 \cdot N \cdot \eta \cdot t / \lim S, \quad (1)$$

where  $N$  is the number of  $^{106}\text{Cd}$  nuclei in the  $^{106}\text{CdWO}_4$  crystal ( $N = 2.42 \times 10^{23}$ ),  $\eta$  is the detection efficiency,  $t$  is the time of measurements, and  $\lim S$  is the number of events of the effect searched for, which can be excluded at a given confidence level (CL). All the limits are presented in this paper with 90% CL.

We have analyzed different data to estimate limits on the  $2\beta$  processes in  $^{106}\text{Cd}$ . For instance, to derive the value of  $\lim S$  for the  $0\nu\varepsilon\beta^+$  decay of  $^{106}\text{Cd}$  to the ground state of  $^{106}\text{Pd}$ , the  $^{106}\text{CdWO}_4$  anticoincidence spectrum was fitted by the model built from the components of the background and the effect searched for. The best fit, achieved in the energy interval 1000 – 3200 keV, gives the area of the effect  $S = 27 \pm 49$  counts, thus providing no evidence for the effect. In accordance with the Feldman-Cousins procedure [42], this corresponds to



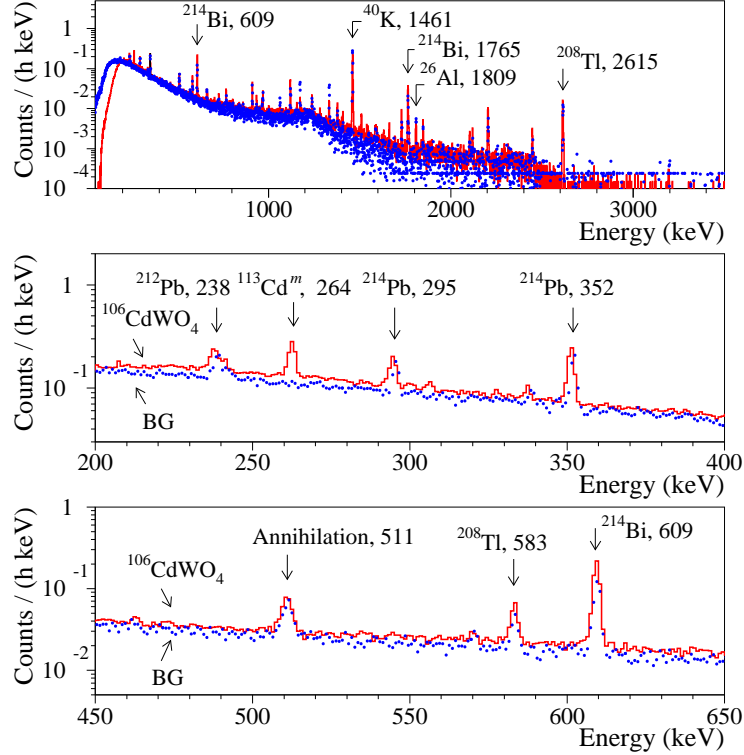


Figure 7: (Color online) Energy spectrum accumulated over 13085 h by the low background HPGe  $\gamma$  detector with the  $^{106}\text{CdWO}_4$  scintillation detector inside (solid red histogram) and background data measured over 4102 h (blue dots). The energy spectra in the 200 – 400 keV (middle part) and 450 – 650 keV (lower part) energy intervals. Energies of  $\gamma$  quanta are in keV.

lim  $S = 107$  counts. Taking into account the detection efficiency within the interval given by the Monte Carlo simulation (69.3%) and the 95.5% efficiency of the pulse-shape discrimination to select  $\gamma$  and  $\beta$  events, we got the half-life limit:  $T_{1/2} \geq 1.5 \times 10^{21}$  yr. The excluded distribution of the  $0\nu\epsilon\beta^+$  decay of  $^{106}\text{Cd}$  to the ground state of  $^{106}\text{Pd}$  is shown in Fig. 6. The limit is lower than that obtained in the previous stage of the experiment [15] due to slightly higher background in the high energy part and worse energy resolution of the  $^{106}\text{CdWO}_4$  detector.

The counting rate of the  $^{106}\text{CdWO}_4$  detector is substantially suppressed in coincidence with the energy 511 keV in the HPGe detectors. The coincidence energy spectrum of the  $^{106}\text{CdWO}_4$  detector is presented in Fig. 9. There are only 115 events in the energy interval 0.05 – 4 MeV, while the simulated background model (built by using the parameters of the anticoincidence spectrum fit) contains 108 counts. We have estimated values of lim  $S$  for the  $2\beta$  processes in  $^{106}\text{Cd}$  in different energy intervals. For instance, there are 62 counts in the energy interval 250 – 1600 keV, while the background model contains 68 counts. According to [42], one should take lim  $S = 8.8$  counts. Taking into account the detection efficiency of the set-up to the  $2\nu\epsilon\beta^+$  decay (7.59%), the part of the energy spectrum in the energy interval (92.3%), the selection efficiency of the pulse-shape discrimination, time and energy cuts used to build the coincidence spectrum (98.4% in total), we have obtained the limit on the  $2\nu\epsilon\beta^+$  decay:  $T_{1/2}^{2\nu\epsilon\beta^+} \geq 2.0 \times 10^{21}$  yr. However, this limit depends on the model of background which has some uncertainty related with our limited knowledge of the radioactive impurities composition

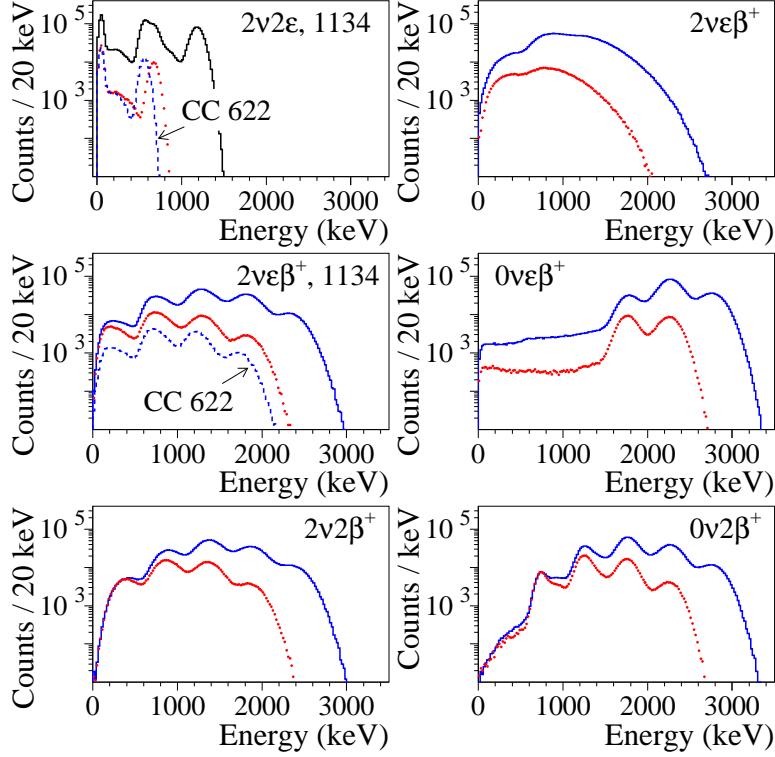


Figure 8: (Color online) Simulated response functions of the  $^{106}\text{CdWO}_4$  detector to  $2\varepsilon$ ,  $\varepsilon\beta^+$ , and  $2\beta^+$  processes in  $^{106}\text{Cd}$  without coincidence (solid histograms) and in coincidence with 511 annihilation  $\gamma$  quanta in the HPGe detector (dotted histograms). Also the response functions of the  $^{106}\text{CdWO}_4$  detector to the  $2\nu 2\varepsilon$  and  $2\nu\varepsilon\beta^+$  decays to the 1134 keV excited level of  $^{106}\text{Pd}$  in coincidence with 622 keV gamma quanta in the HPGe detector are shown by dashed histograms.

and localization in the set-up. In addition, in some energy intervals (as in the considered above 250 – 1600 keV) the measured number of events is less than in the model of background. The authors of work [42] suggest in such a situation to report the so called "sensitivity" of the experiment defined as the average upper limit that would be obtained by an ensemble of experiments with the expected background and no true signal. Following these suggestions we took a more conservative, background model independent limit on the number of events of the effect searched for as  $\lim S = 15.3$  counts, which leads to the following half-life limit on the  $2\nu\varepsilon\beta^+$  decay of  $^{106}\text{Cd}$  to the ground state of  $^{106}\text{Pd}$  which we accept as a final result:

$$T_{1/2}^{2\nu\varepsilon\beta^+} \geq 1.1 \times 10^{21} \text{ yr.}$$

The excluded distribution of the  $2\nu\varepsilon\beta^+$  decay of  $^{106}\text{Pd}$  to the ground state of  $^{106}\text{Pd}$  is presented in Fig. 9 together with the excluded spectra of the neutrinoless and two neutrino double positron decay of  $^{106}\text{Cd}$ . The limits on the processes with positron(s) emission for transitions to the ground and excited states of  $^{106}\text{Pd}$  were obtained in a similar way mainly by using the coincidence of the  $^{106}\text{CdWO}_4$  detector with annihilation  $\gamma$  quanta in the HPGe detectors (the limits are presented in Table 1). A rather high sensitivity was achieved for the  $\varepsilon\beta^+$  and  $2\beta^+$

decay channels thanks to the comparatively high probability to detect at least one annihilation gamma quantum by the HPGe counters (e.g., 13.6% for the  $2\beta^+$  decay).

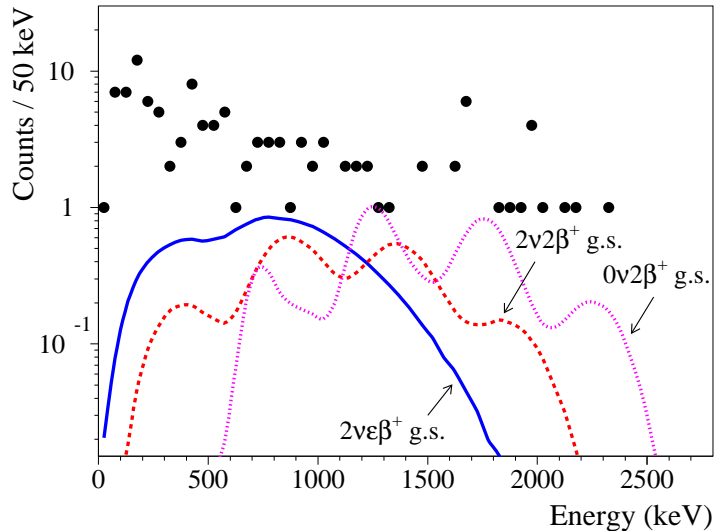


Figure 9: (Color online) Energy spectrum of the  $^{106}\text{CdWO}_4$  detector in coincidence with 511 keV annihilation  $\gamma$  quanta in at least one of the HPGe detectors (filled circles) acquired over 13085 h. The excluded distributions of different  $2\beta$  processes in  $^{106}\text{Cd}$  are shown by different lines.

Further suppression of the background was achieved by selection of events in the  $^{106}\text{CdWO}_4$  detector in coincidence with the intense  $\gamma$  quanta in the HPGe counters expected in the double electron capture in  $^{106}\text{Cd}$  to the excited levels of  $^{106}\text{Pd}$ . For instance, gamma quanta with energy 616 keV expected in the  $2\varepsilon$  decay of  $^{106}\text{Cd}$  to the excited level 1128 keV of  $^{106}\text{Pd}$  can be detected by the HPGe counters with a detection efficiency 2.42% (2.34%) in the two neutrino (neutrinoless) process. As one can see in Fig. 10, there are only 17 (23) counts in the energy interval 50 – 700 keV (50 – 2500 keV). According to [42] one should take a "sensitivity" estimation of  $\lim S = 8.4(9.7)$  counts. The energy intervals contain 78.2% (86.2%) of the simulated  $2\nu 2\varepsilon$  ( $0\nu 2\varepsilon$ ) spectra. Taking into account the efficiency of the pulse-shape discrimination, the time and energy coincidence with the gamma quanta 616 keV (97.3% in total), the following half-life limit on the  $2\nu 2\varepsilon$  ( $0\nu 2\varepsilon$ ) decay of  $^{106}\text{Cd}$  to the excited level 1128 keV of  $^{106}\text{Pd}$  can be obtained:  $T_{1/2}^{2\nu 2\varepsilon} \geq 5.5 \times 10^{20}$  yr ( $T_{1/2}^{0\nu 2\varepsilon} \geq 5.1 \times 10^{20}$  yr). The excluded distributions of the  $2\nu 2\varepsilon$  and  $0\nu 2\varepsilon$  decays of  $^{106}\text{Cd}$  to the 1128 keV excited level of  $^{106}\text{Pd}$  are presented in Fig. 10.

Most of the limits on the double electron capture in  $^{106}\text{Cd}$  to the excited levels of  $^{106}\text{Pd}$  were obtained in a similar way (including the transitions to the levels of  $^{106}\text{Pd}$  with energies 2718 keV and 2748 keV where the resonant processes are possible). Typical detection efficiencies for the  $2\varepsilon$  processes in  $^{106}\text{Cd}$  to the excited levels of  $^{106}\text{Pd}$  are 1.17% – 4.13% depending on the level and decay mode, while the number of counts varies from 83 to 0 depending on the energy in the HPGe detectors chosen to build the coincidence spectra. For example, 83 coincidence counts were obtained in the energy interval 50 – 2600 keV in CC with energy 512 keV in the HPGe counters, while 0 events were detected in the energy interval 650 – 2000 keV in the coincidence with the energy 1160 keV in the HPGe detectors (resonant  $0\nu 2K$  capture to the

2718 keV excited level of  $^{106}\text{Pd}$ ).

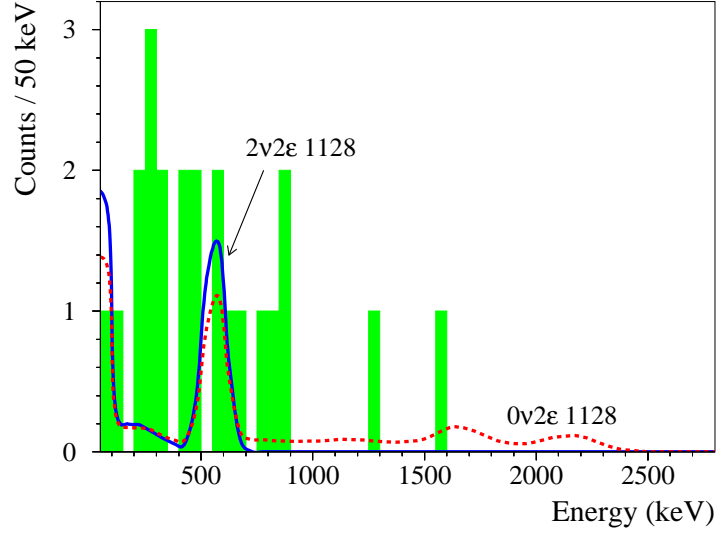


Figure 10: (Color online) Energy spectrum of the  $^{106}\text{CdWO}_4$  detector in coincidence with 616 keV  $\gamma$  quanta in the HPGe detector (filled histogram) acquired over 13085 h. The excluded distributions of the  $2\nu 2\varepsilon$  and  $0\nu 2\varepsilon$  decay of  $^{106}\text{Cd}$  to the 1128 keV excited level of  $^{106}\text{Pd}$  with detection of 616 keV  $\gamma$  quanta in the HPGe detectors are shown.

We have also used the data accumulated by the HPGe detectors to estimate limits on the  $2\beta$  processes in  $^{106}\text{Cd}$ . For instance, in neutrinoless  $2\varepsilon$  capture we assume that the energy excess is taken away by bremsstrahlung  $\gamma$  quanta with energy  $E_\gamma = Q_{2\beta} - E_{b1} - E_{b2} - E_{exc}$ , where  $E_{bi}$  is the binding energy of  $i$ -th captured electron on the atomic shell, and  $E_{exc}$  is the energy of the populated (g.s. or excited) level of  $^{106}\text{Pd}$ . In case of transition to an excited level, in addition to the initial  $\gamma$  quantum, other  $\gamma$ 's will be emitted in the nuclear deexcitation process. For example, to derive a limit on the  $0\nu 2K$  capture in  $^{106}\text{Cd}$  to the ground state of  $^{106}\text{Pd}$  the energy spectrum accumulated with the HPGe detectors was fitted in the energy interval 2700 – 2754 keV by a simple function (first degree polynomial function to describe background plus Gaussian peak at the energy 2726.7 keV with the energy resolution  $\text{FWHM} = 4.4$  keV to describe the effect searched for). The fit gives an area of the peak  $6.2 \pm 3.2$  counts, with no evidence for the effect. According to [42] we took 11.4 events which can be excluded with 90% CL. Taking into account the detection efficiency for gamma quanta with energy 2726.7 keV in the experimental conditions (1.89%) we have set the following limit for the  $0\nu 2K$  capture of  $^{106}\text{Cd}$  to the ground state of  $^{106}\text{Pd}$ :  $T_{1/2} \geq 4.2 \times 10^{20}$  yr. Limits on the  $0\nu KL$  and  $0\nu 2L$  capture in  $^{106}\text{Cd}$  to the ground state of  $^{106}\text{Pd}$  ( $T_{1/2} \geq 1.3 \times 10^{21}$  yr and  $T_{1/2} \geq 5.4 \times 10^{20}$  yr, respectively) were derived in the similar way. The excluded peaks are shown in Fig. 11. We would like to stress the certain advantages of isotope  $^{106}\text{Cd}$  for which the high accuracy  $Q_{2\beta}$  value is now available. Thanks to this feature one could distinguish clearly the  $0\nu 2K$ ,  $0\nu KL$  and  $0\nu 2L$  modes of the decay using high resolution HPGe detectors.

All the half-life limits obtained in the present work are summarized in Table 1, where results of the most sensitive previous experiments are given for comparison.

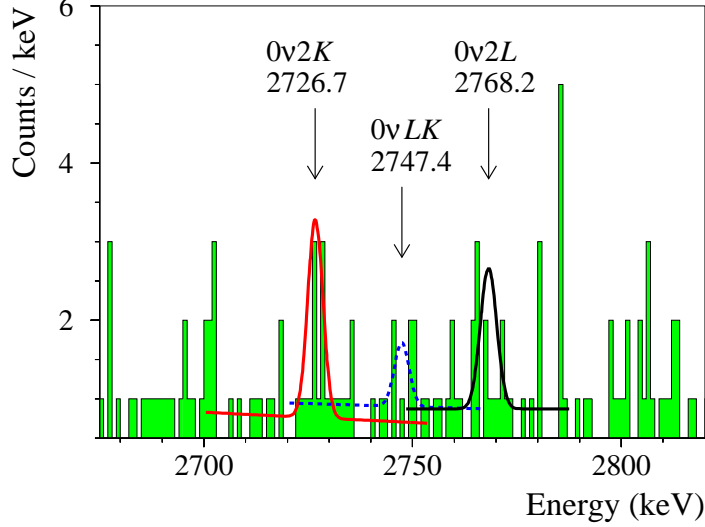


Figure 11: (Color online) Part of the energy spectrum accumulated by the HPGe detector. Excluded peaks expected in the  $0\nu 2K$ ,  $0\nu LK$  and  $0\nu 2L$  capture in  $^{106}\text{Cd}$  to the ground state of  $^{106}\text{Pd}$  are shown. Energies of the expected  $\gamma$  peaks are in keV.

### 3.2.1 Limit on $^{106}\text{Cd}$ $2\nu\varepsilon\beta^+$ decay matrix element

An upper limit on the effective nuclear matrix element for the  $2\nu\varepsilon\beta^+$  decay ( $M_{eff}^{2\nu\varepsilon\beta^+}$ ) can be obtained with the help of the following formula:

$$\lim M_{eff}^{2\nu\varepsilon\beta^+} = 1/\sqrt{\lim T_{1/2}^{2\nu\varepsilon\beta^+} G^{2\nu\varepsilon\beta^+}}, \quad (2)$$

where  $G^{2\nu\varepsilon\beta^+}$  is the phase space factor for the  $2\nu\varepsilon\beta^+$  decay,  $M_{eff}^{2\nu\varepsilon\beta^+} = g_A^2(m_e c^2)M^{2\nu\varepsilon\beta^+}$ ,  $g_A$  is the axial vector coupling constant, and  $m_e c^2$  is the electron mass. Using the recently calculated phase space factors  $702 \times 10^{-24} \text{ yr}^{-1}$  [43] and  $741 \times 10^{-24} \text{ yr}^{-1}$  [44], we have obtained the following limit on the nuclear matrix element for the  $2\nu\varepsilon\beta^+$  decay of  $^{106}\text{Cd}$  to the ground state of  $^{106}\text{Pd}$ :  $M_{eff}^{2\nu\varepsilon\beta^+} \leq 1.1$ .

## 4 CONCLUSIONS

An experiment to search for  $2\beta$  decay of  $^{106}\text{Cd}$  with enriched  $^{106}\text{CdWO}_4$  crystal scintillator in coincidence with four crystals HPGe  $\gamma$  detector has been completed after 13085 h of data taking. New limits on  $2\varepsilon$ ,  $\varepsilon\beta^+$  and  $2\beta^+$  processes in  $^{106}\text{Cd}$  were set on the level of  $T_{1/2} > 10^{20} - 10^{21} \text{ yr}$ . The highest sensitivity was achieved mainly by analysis of coincidence between the  $^{106}\text{CdWO}_4$  and the HPGe detectors. For the decay channels with emission of positrons ( $\varepsilon\beta^+$  and  $2\beta^+$  decays) a higher sensitivity was achieved in coincidence with annihilation gamma quanta, while coincidence of the  $^{106}\text{CdWO}_4$  detector with intensive gamma quanta in the HPGe counters gives the most stringent limits on the double electron capture in  $^{106}\text{Cd}$  to excited levels of  $^{106}\text{Pd}$ . The half-life limit on the two neutrino  $\varepsilon\beta^+$  decay,  $T_{1/2} \geq 1.1 \times 10^{21} \text{ yr}$ , reached the region of some theoretical predictions [19, 46, 47, 48, 49, 50]. By using the half-life limit the nuclear matrix element for the  $2\nu\varepsilon\beta^+$  decay of  $^{106}\text{Cd}$  to the ground state of  $^{106}\text{Pd}$  can be bounded as

Table 1: Half-life limits on  $2\beta$  processes in  $^{106}\text{Cd}$ . The experimental selection (AC anticoincidence, CC in coincidence at the given energy with HPGe, HPGe using only the HPGe detectors) is also reported. The results of the most sensitive previous experiments are given for comparison.

Decay channel	Decay mode	Level of $^{106}\text{Pd}$ (keV)	$T_{1/2}$ limit (yr) at 90% C.L.	
			Present work (Data)	Best previous limit
$2\varepsilon$	$2\nu$	g.s.	–	$\geq 4.2 \times 10^{20}$ [25]
$2\varepsilon$	$2\nu$	$2^+$ 512	$\geq 9.9 \times 10^{20}$ (CC 512 keV)	$\geq 1.2 \times 10^{20}$ [25]
$2\varepsilon$	$2\nu$	$2^+$ 1128	$\geq 5.5 \times 10^{20}$ (CC 616 keV)	$\geq 4.1 \times 10^{20}$ [15]
$2\varepsilon$	$2\nu$	$0^+$ 1134	$\geq 1.0 \times 10^{21}$ (CC 622 keV)	$\geq 1.7 \times 10^{20}$ [15]
$2\varepsilon$	$2\nu$	$2^+$ 1562	$\geq 7.4 \times 10^{20}$ (CC 1050 keV)	$\geq 5.1 \times 10^{19}$ [15]
$2\varepsilon$	$2\nu$	$0^+$ 1706	$\geq 7.1 \times 10^{20}$ (CC 1194 keV)	$\geq 1.1 \times 10^{20}$ [15]
$2\varepsilon$	$2\nu$	$0^+$ 2001	$\geq 9.7 \times 10^{20}$ (CC 873 keV)	$\geq 2.9 \times 10^{20}$ [15]
$2\varepsilon$	$2\nu$	$0^+$ 2278	$\geq 1.0 \times 10^{21}$ (CC 1766 keV)	$\geq 1.6 \times 10^{20}$ [15]
$2K$	$0\nu$	g.s.	$\geq 4.2 \times 10^{20}$ (HPGe)	$\geq 1.0 \times 10^{21}$ [15]
$LK$	$0\nu$	g.s.	$\geq 1.3 \times 10^{21}$ (HPGe)	$\geq 1.0 \times 10^{21}$ [15]
$2L$	$0\nu$	g.s.	$\geq 5.4 \times 10^{20}$ (HPGe)	$\geq 1.0 \times 10^{21}$ [15]
$2\varepsilon$	$0\nu$	$2^+$ 512	$\geq 3.9 \times 10^{20}$ (CC 512 keV)	$\geq 5.1 \times 10^{20}$ [15]
$2\varepsilon$	$0\nu$	$2^+$ 1128	$\geq 5.1 \times 10^{20}$ (CC 616 keV)	$\geq 3.1 \times 10^{20}$ [15]
$2\varepsilon$	$0\nu$	$0^+$ 1134	$\geq 1.1 \times 10^{21}$ (CC 622 keV)	$\geq 3.5 \times 10^{20}$ [15]
$2\varepsilon$	$0\nu$	$2^+$ 1562	$\geq 7.3 \times 10^{20}$ (CC 1050 keV)	$\geq 3.5 \times 10^{20}$ [15]
$2\varepsilon$	$0\nu$	$0^+$ 1706	$\geq 1.0 \times 10^{21}$ (CC 1194 keV)	$\geq 2.5 \times 10^{20}$ [15]
$2\varepsilon$	$0\nu$	$0^+$ 2001	$\geq 1.2 \times 10^{21}$ (CC 873 keV)	$\geq 2.3 \times 10^{20}$ [15]
$2\varepsilon$	$0\nu$	$0^+$ 2278	$\geq 8.6 \times 10^{20}$ (CC 1766 keV)	$\geq 2.1 \times 10^{20}$ [15]
Res. $2K$	$0\nu$	2718	$\geq 1.1 \times 10^{21}$ (CC 1160 keV)	$\geq 4.3 \times 10^{20}$ [15]
Res. $KL_1$	$0\nu$	$4^+$ 2741	$\geq 8.5 \times 10^{20}$ (HPGe)	$\geq 9.5 \times 10^{20}$ [15]
Res. $KL_3$	$0\nu$	$2, 3^-$ 2748	$\geq 1.4 \times 10^{21}$ (CC 2236 keV)	$\geq 4.3 \times 10^{20}$ [15]
$\varepsilon\beta^+$	$2\nu$	g.s.	$\geq 1.1 \times 10^{21}$ (CC 511 keV)	$\geq 4.1 \times 10^{20}$ [45]
$\varepsilon\beta^+$	$2\nu$	$2^+$ 512	$\geq 1.3 \times 10^{21}$ (CC 511 keV)	$\geq 2.6 \times 10^{20}$ [45]
$\varepsilon\beta^+$	$2\nu$	$2^+$ 1128	$\geq 1.0 \times 10^{21}$ (CC 511 keV)	$\geq 3.1 \times 10^{20}$ [15]
$\varepsilon\beta^+$	$2\nu$	$0^+$ 1134	$\geq 1.1 \times 10^{21}$ (CC 622 keV)	$\geq 3.7 \times 10^{20}$ [15]
$\varepsilon\beta^+$	$0\nu$	g.s.	$\geq 1.5 \times 10^{21}$ (AC)	$\geq 2.2 \times 10^{21}$ [15]
$\varepsilon\beta^+$	$0\nu$	$2^+$ 512	$\geq 1.9 \times 10^{21}$ (CC 511 keV)	$\geq 1.3 \times 10^{21}$ [15]
$\varepsilon\beta^+$	$0\nu$	$2^+$ 1128	$\geq 1.3 \times 10^{21}$ (CC 511 keV)	$\geq 5.7 \times 10^{20}$ [15]
$\varepsilon\beta^+$	$0\nu$	$0^+$ 1134	$\geq 1.9 \times 10^{21}$ (CC 622 keV)	$\geq 5.0 \times 10^{20}$ [15]
$2\beta^+$	$2\nu$	g.s.	$\geq 2.3 \times 10^{21}$ (CC 511 keV)	$\geq 4.3 \times 10^{20}$ [15]
$2\beta^+$	$2\nu$	$2^+$ 512	$\geq 2.5 \times 10^{21}$ (CC 511 keV)	$\geq 5.1 \times 10^{20}$ [15]
$2\beta^+$	$0\nu$	g.s.	$\geq 3.0 \times 10^{21}$ (CC 511 keV)	$\geq 1.2 \times 10^{21}$ [15]
$2\beta^+$	$0\nu$	$2^+$ 512	$\geq 2.5 \times 10^{21}$ (CC 511 keV)	$\geq 1.2 \times 10^{21}$ [15]

$M_{eff}^{2\nu\varepsilon\beta^+} \leq 1.1$ . The resonant neutrinoless double electron captures to the 2718 keV, 2741 keV and 2748 keV excited states of  $^{106}\text{Pd}$  are restricted on the level of  $T_{1/2} \geq (8.5 \times 10^{20} - 1.4 \times 10^{21})$

yr. Unfortunately, the experiment has no competitive sensitivity to the most probable  $2\nu 2K$  channel of the decay due to the high activity of  $^{113}\text{Cd}^m$  in the  $^{106}\text{CdWO}_4$  crystal scintillator. Advancement of the experiment is in progress using the  $^{106}\text{CdWO}_4$  detector in coincidence with two large volume  $\text{CdWO}_4$  scintillation detectors in close geometry to improve the detection efficiency to gamma quanta emitted in the double beta processes in  $^{106}\text{Cd}$ .

## 5 ACKNOWLEDGMENTS

The authors from the Institute for Nuclear Research (Kyiv, Ukraine) were supported in part by the project CO-1-2/2015 of the Program of collaboration with the Joint Institute for Nuclear Research (Dubna) "Promising basic research on High Energy and Nuclear Physics" for 2014-2015 of the National Academy of Sciences of Ukraine. We are grateful to S.R. Elliott for his note on presence of  $^{116}\text{Cd}$   $2\nu 2\beta^-$  decay in  $^{106}\text{CdWO}_4$  data. We would like to thank Prof. H. Ejiri for useful discussions.

## References

- [1] J.D. Vergados, H. Ejiri, F. Šimkovic, Theory of neutrinoless double-beta decay, *Rep. Prog. Phys.* **75**, 106301 (2012).
- [2] J. Barea, J. Kotila, F. Iachello, Limits on Neutrino Masses from Neutrinoless Double- $\beta$  Decay, *Phys. Rev. Lett.* **109**, 042501 (2012).
- [3] W. Rodejohann, Neutrino-less double beta decay and particle physics, *J. Phys. G* **39**, 124008 (2012).
- [4] F.F. Deppisch, M. Hirsch, H. Päs, Neutrinoless double-beta decay and physics beyond the standard model, *J. Phys. G* **39**, 124007 (2012).
- [5] S.M. Bilenky, C. Giunti, Neutrinoless double-beta decay: A probe of physics beyond the Standard Model, *Int. J. Mod. Phys. A* **30**, 1530001 (2015).
- [6] V.I. Tretyak, Yu.G. Zdesenko, Tables of double beta decay data, *At. Data Nucl. Data Tables* **61**, 43 (1995).
- [7] V.I. Tretyak, Yu.G. Zdesenko, Tables of double  $\beta$  decay data – an update, *At. Data Nucl. Data Tables* **80**, 83 (2002).
- [8] S.R. Elliott, Recent progress in double beta decay, *Mod. Phys. Lett. A* **27**, 1230009 (2012).
- [9] A. Giuliani, A. Poves, Neutrinoless Double-Beta Decay, *AHEP* **2012**, 857016 (2012).
- [10] R. Saakyan, Two-Neutrino Double-Beta Decay, *Annu. Rev. Nucl. Part. Sci.* **63**, 503 (2013).
- [11] O. Cremonesi, M. Pavan, Challenges in Double Beta Decay, *AHEP* **2014**, 951432 (2014).
- [12] J.J. Gómez-Cadenas and J. Martín-Albo, Phenomenology of Neutrinoless Double Beta Decay, *Proc. of Sci. (GSSI14)*, 004 (2015).

- [13] X. Sarazin, Review of Double Beta Experiments, J. Phys.: Conf. Ser. **593**, 012006 (2015).
- [14] J. Maalampi, J. Suhonen, Neutrinoless Double  $\beta^+$ /EC Decays, AHEP **2013**, 505874 (2013).
- [15] P. Belli et al., Search for double- $\beta$  decay processes in  $^{106}\text{Cd}$  with the help of a  $^{106}\text{CdWO}_4$  crystal scintillator, Phys. Rev. C **85**, 044610 (2012).
- [16] A.P. Meshik et al., Weak decay of  $^{130}\text{Ba}$  and  $^{132}\text{Ba}$ : Geochemical measurements, Phys. Rev. C **64**, 035205 (2001).
- [17] M. Pujol et al., Xenon in Archean barite: Weak decay of  $^{130}\text{Ba}$ , mass-dependent isotopic fractionation and implication for barite formation, Geochim. Cosmochim. Acta **73**, 6834 (2009).
- [18] Yu.M. Gavriluk et al., Indications of  $2\nu 2K$  capture in  $^{78}\text{Kr}$ , Phys. Rev. C **87**, 035501 (2013).
- [19] M. Hirsch et al., Nuclear structure calculation of  $\beta^+\beta^+$ ,  $\beta^+/\text{EC}$  and  $\text{EC}/\text{EC}$  decay matrix elements, Z. Phys. A **347**, 151 (1994).
- [20] M. Wang et al., The AME2012 atomic mass evaluation (II). Tables, graphs and references, Chinese Phys. C **36**, 1603 (2012).
- [21] M. Berglund, M.E. Wieser, Isotopic compositions of the elements 2009 (IUPAC Technical Report), Pure Appl. Chem. **83**, 397 (2011).
- [22] M.I. Krivoruchenko et al., Resonance enhancement of neutrinoless double electron capture, Nucl. Phys. A **859**, 140 (2011).
- [23] D. De Frenne, A. Negret, Nuclear Data Sheets for  $A = 106$ , Nucl. Data Sheets **109**, 943 (2008).
- [24] N.I. Rukhadze et al., New limits on double beta decay of  $^{106}\text{Cd}$ , Nucl. Phys. A **852**, 197 (2011).
- [25] N.I. Rukhadze et al., Search for double beta decay of  $^{106}\text{Cd}$ , Bull. Russ. Acad. Sci. Phys. **75**, 879 (2011).
- [26] Ch. Briancon et al., New Search for Double Electron Capture in  $^{106}\text{Cd}$  Decay with the TGV-2 Spectrometer, Phys. At. Nucl. **78**, 740 (2015).
- [27] J. Ebert et al., Current Status and Future Perspectives of the COBRA Experiment, AHEP **2013**, 703572 (2013).
- [28] P. Belli et al., Development of enriched  $^{106}\text{CdWO}_4$  crystal scintillators to search for double  $\beta$  decay processes in  $^{106}\text{Cd}$ , Nucl. Instr. Meth. A **615**, 301 (2010).
- [29] V.I. Tretyak et al., First results of the experiment to search for  $2\beta$  decay of  $^{106}\text{Cd}$  with  $^{106}\text{CdWO}_4$  crystal scintillator in coincidence with four crystals HPGe detector, EPJ Web of Conferences **65**, 01003 (2014).



- [30] O.G. Polischuk et al., Search for  $2\beta$  processes in  $^{106}\text{Cd}$  with  $^{106}\text{CdWO}_4$  crystal scintillator, *Functional Materials* **22**, 135 (2015).
- [31] F.A. Danevich et al., Search for double beta processes in  $^{106}\text{Cd}$  with enriched  $^{106}\text{CdWO}_4$  crystal scintillator in coincidence with four crystals HPGe detector, *AIP Conf. Proc.* **1686**, 020006 (2015).
- [32] V.I. Tretyak et al., New limits on  $2\beta$  processes in  $^{106}\text{Cd}$ , to be published in *Proceedings of the TAUP 2015 conference, September 2015*, *J. Phys.: Conf. Ser.* (2016), edited by Institute of Physics Publishing (IoP).
- [33] R.S. Boiko et al., Ultrapurification of archaeological lead, *Inorganic Materials* **47**, 645 (2011).
- [34] F.A. Danevich et al., Ancient Greek lead findings in Ukraine, *Nucl. Instr. Meth. A* **603**, 328 (2009).
- [35] M. Laubenstein et al., Underground measurements of radioactivity, *Appl. Radiat. Isotopes* **61**, 167 (2004).
- [36] F.A. Danevich et al., Development of radiopure cadmium tungstate crystal scintillators from enriched  $^{106}\text{Cd}$  and  $^{116}\text{Cd}$  to search for double beta decay, *AIP Conf. Proc.* **1549**, 201 (2013).
- [37] W.R. Nelson et al., The EGS4 code system, SLAC-Report-265 (Stanford, 1985).
- [38] L. Bardelli et al., Pulse-shape discrimination with  $\text{PbWO}_4$  crystal scintillators, *Nucl. Instr. Meth. A* **584**, 129 (2008).
- [39] L. Bardelli et al., Further study of  $\text{CdWO}_4$  crystal scintillators as detectors for high sensitivity  $2\beta$  experiments: Scintillation properties and pulse-shape discrimination, *Nucl. Instr. Meth. A* **569**, 743 (2006).
- [40] F.A. Danevich et al., Search for double beta decay of  $^{116}\text{Cd}$  with enriched  $^{116}\text{CdWO}_4$  crystal scintillators (Aurora experiment), to be published in *Proceedings of the TAUP 2015 conference, September 2015*, *J. Phys.: Conf. Ser.* (2016), edited by Institute of Physics Publishing (IoP).
- [41] J. Blachot, Nucl. Data Sheets for  $A = 113$ , *Nucl. Data Sheets* **111**, 1471 (2010).
- [42] G.J. Feldman, R.D. Cousins, Unified approach to the classical statistical analysis of small signals, *Phys. Rev. D* **57**, 3873 (1998).
- [43] J. Kotila, F. Iachello, Phase space factors for  $\beta^+\beta^+$  decay and competing modes of double- $\beta$  decay, *Phys. Rev. C* **87**, 024313 (2013).
- [44] M. Mirea, T. Pahomi, S. Stoica, Values of the phase space factors involved in double beta decay, *Romanian Reports in Physics* **67**, 872 (2015).
- [45] P. Belli et al., New limits on  $2\beta^+$  decay processes in  $^{106}\text{Cd}$ , *Astropart. Phys.* **10**, 115 (1999).

- [46] A.S. Barabash et al., Theoretical and experimental investigation of the double beta processes in  $^{106}\text{Cd}$ , Nucl. Phys. A **604**, 115 (1996).
- [47] J. Toivanen, J. Suhonen, Study of several double-beta-decaying nuclei using the renormalized proton-neutron quasiparticle random-phase approximation, Phys. Rev. C **55**, 2314 (1997).
- [48] O.A. Romyantsev, M.H. Urin, The strength of the analog and Gamow-Teller giant resonances and hindrance of the  $2\nu\beta\beta$ -decay rate, Phys. Lett. B **443**, 51 (1998).
- [49] O. Civitarese, J. Suhonen, Is the single-state dominance realized in double- $\beta$ -decay transitions?, Phys. Rev. C **58**, 1535 (1998).
- [50] J. Suhonen, O. Civitarese, Theoretical results on the double positron decay of  $^{106}\text{Cd}$ , Phys. Lett. B **497**, 221 (2001).